Cylindrical and Spherical Shells with Cracks*

F. ERDOGAN AND J. J. KIBLER

Department of Mechanical Engineering and Mechanics, Lehigh University, Bethlehem, Pa.

The symmetric problem for the cylindrical and spherical shells containing a meridional crack is considered. The problem is solved for a uniform membrane load and a uniform bending moment applied to the surface of the crack. The extensional and bending components of the stress intensity factor ratio are obtained as functions of shell parameter and are tabulated. The results are also plotted in order to compare them with the existing asymptotic solutions.

Introduction

A meridional crack in cylindrical and spherical shells subjected to internal pressure was considered by Folias [1, 2]. After obtaining the respective systems of integral equations for the cylinder and the sphere, Folias gave asymptotic expressions for the stress intensity factors for both cases. These expressions are valid only for small values of shell parameter λ, hence their range of application is limited. In this paper, the integral equations are solved numerically and the stress intensity factors are evaluated for up to $\lambda = 8$ in cylindrical shells and up to $\lambda = 5$ in spherical shells.

The Solution and Results

To analyze the stress singularities at the ends of meridional cracks in isotropic and homogeneous thin shells, in refs. [1] and [2], the following linearized shallow shell equations were used, which are due to Marguerre [3] and Reissner [4]:

$$\frac{Eha^2}{R} \frac{\partial^2 W}{\partial x^2} + \nabla^4 F = 0$$

$$\nabla^4 W - \frac{a^2}{RD} \frac{\partial^2 F}{\partial x^2} = \frac{q}{D} a^4$$

(1)

for cylindrical shells, and

$$-\frac{Eha^2}{R} \nabla^2 W + \nabla^4 F = 0$$

$$\nabla^4 W + \frac{a^2}{RD} \nabla^2 F = \frac{q}{D} a^4$$

(2)

for spherical shells. In (1) and (2), X, Y, Z are the rectangular coordinates with Z normal to the surface and X in the plane of the crack, W is the displacement in Z-direction, $x = X/a$, $y = Y/a$ are dimensionless coordinates, a is the half-crack length, R is the mean radius, h is the shell thickness, F is the stress function, q is the normal traction acting on the shell surface, E is the Young's modulus and D is the flexural rigidity, $D = Eh^3/12(1 - v^2)$, v being the Poisson's ratio. In the usual manner, the components of bending moment M_x, M_y, M_{xy} and transverse shear Q_x, Q_y are given in terms of W and the membrane forces N_x, N_y, N_{xy} are given in terms of F.

In general, the singular solution of the cracked shell problem may be reduced to a pertur-
bation problem in which self-equilibrating forces and moments acting on the crack surfaces
are the only external loads. Thus, in one class of important symmetric problems, the homogene-
ous systems obtained from (1) and (2) will have to be solved with the following boundary
conditions on the crack surface

$$M_y = M_0(x), \quad V_y = Q_y + \frac{\partial M_{xy}}{\partial x} = 0,$$

$$N_y = N_0(x), \quad N_{xy} = 0, \quad (-1 < x < 1, \ y = 0)$$

(3)

and vanishing stresses away from the crack. Due to the conditions of symmetry, in refs. [1]
and [2], the functions $F(x, y)$ and $W(x, y)$ are expressed in terms of Fourier cosine integrals,
and the resulting dual integral equations are reduced to a system of singular integral equations
of the following form*

$$\int_{-1}^{1} \sum_{1}^{2} h_{ij}(x, t) u_j(t) \mathrm{d}t = f_i(x), \qquad (i = 1, 2; \ -1 < x < 1)$$

(4)

where the kernels h_{ij} contain Cauchy-type singularities, u_1, u_2 are conveniently defined un-
known functions and f_1, f_2 are related to the external loads. For example, for constant M_y
and N_y in (3), letting

$$M_0 = \frac{m_0 D}{a^2}, \quad N_0 = \frac{n_0}{a^2}$$

(5)

we have

$$f_1(x) = \frac{\pi n_0}{i(EDh)^{\frac{1}{2}}} x, \quad f_2(x) = -\pi m_0 x.$$

(6)

The kernels $h_{ij}(x, t)$ in (4) contain modified Bessel functions of the form, $K_j(e^{\mp \pi i/4}|t - x|\lambda/n)$,
$(j = 0, 1)$, where $n = 2$ for cylindrical shells, $n = 1$ for spherical shells and λ is the shell parameter
defined by

$$\lambda = [12(1 - v^2)]^{\frac{1}{4}} \frac{a}{(Rh)^{\frac{1}{2}}}.$$

Here v is the Poisson's ratio, a is the half-crack length, R is shell radius of curvature and h
is the shell thickness.

Studying the asymptotic values of the kernels for small arguments, it is easily shown that
at $t = x$, h_{ij} are singular and the leading terms are of the form $a_{ij}/(t - x)$, where a_{ij}, $(i, j = 1, 2)$,
are constant. For convenience in the numerical analysis, we replace the modified Bessel
functions having complex arguments by the Kelvin functions with real arguments by using
the following relation:

$$e^{-\frac{1}{2} v \pi i} K_v(x e^{\pi i/4}) = ker_v x + i kei_v x.$$

(7)

Around zero, the functions ker_1 and kei_1 behave like $1/x$ which provide the singularity of the
integral equations and may easily be separated. By using the polynomial approximations for
the functions ker_v and kei_v, $(v = 1, 2)$ given in ref. [7], (4) may be put in the following form:

$$\int_{-1}^{1} \sum_{1}^{2} a_{ij} u_j(t) \frac{\mathrm{d}t}{t - x} + \int_{-1}^{1} k_{ij}(x, t) u_j(t) \mathrm{d}t = f_i(x) \qquad i = 1, 2, \ |x| < 1$$

(8)

where the coefficients a_{ij} are known constants and the kernels k_{ij} are bounded known functions.

From the definitions of the auxiliary functions u_1 and u_2 as given in refs. [1] and [2], it can
be shown that u_1 and u_2 are even functions and the index of the system of equations (8) is -1,
that is, u_1 and u_2 may be expressed as

---

* For details of the analysis and explicit forms of the kernels h_{ij}, see refs. [5] and [6].

$$u_j(x) = (1-x^2)^{\frac{1}{2}} A_j(x^2), \qquad (j=1, 2) \tag{9}$$

where the functions A_1, A_2 are regular. Again, referring to refs. [1] and [2] for details, we simply note that the extensional and beinding components of the stress intensity factors are directly related to the values of the functions A_j at $x=1$. Hence the solution of (8) is sufficient for the evaluation of stress intensity factors.

The system of singular integral equations (8) may be regularized by using the method of Muskhelishvili [8] or Carlemann and Vekua [9]. However, because of the complexity of the kernels k_{ij}, the process is quite complicated and the solution of the resulting system of integral equations with weakly singular kernels can only be solved approximately. Therefore, to solve (8), we use the method described in ref. [10], which is based on the observation that the fundamental function of the system (8) is the weight of Chebishev polynomials. Thus, the singularities of (8) may be removed by expressing the functions A_j as infinite series in these orthogonal polynomials. The technique is rather easy to apply and allows introducing into the program an automatic convergence scheme for a desired degree of accuracy in the computed quantities (by simply specifying the number of significant digits in stress intensity ratios which should be repeated as the number of terms in the series is increased).

Here, we give the numerical results for four different cases, namely the cylindrical and the spherical shells with the loading conditions $N_0 \neq 0$, $M_0 = 0$ and $N_0 = 0$, $M_0 \neq 0$. Let the stress intensity factors in shells be

$$
\begin{aligned}
k_s &= (A_e + A_b)k_p \quad \text{(outer surface)} \\
k_s &= (A_e - A_b)k_p \quad \text{(inner surface)}
\end{aligned}
\tag{10}
$$

TABLE 1

Stress intensity factor ratios for $N_0 \neq 0$, $M_0 = 0$

λ	Cylinder		Sphere	
	A_e	a_b	A_e	a_b
0.2	1.0096	0.00410	1.0112	0.00611
0.4	1.0371	0.01124	1.0422	0.01693
0 6	1.0795	0.01902	1.0887	0.02919
0.8	1.1344	0.02659	1.1479	0.04186
1.0	1.1993	0.03359	1.2174	0.05448
1.2	1.2723	0.03985	1.2956	0.06685
1.4	1.3519	0.04529	1.3812	0.07886
1.6	1 4367	0.04990	1.4731	0.09045
1.8	1.5256	0.05368	1.5706	0.10155
2.0	1.6177	0.05664	1.6729	0.11216
2.2	1.7122	0.05883	1.7795	0.12223
2.4	1.8085	0.06018	1.8899	0.13172
2.6	1.9060	0.06090	2.0038	0.14058
2.8	2.0045	0.06083	2.1208	0.14879
3.0	2.1035	0.06014	2.2408	0.15630
3.25	2.2276	0.05832	2.3947	0.16463
3.50	2.3519	0.05549	2.5526	0.17172
3.75	2.4761	0.05172	2.7143	0.17751
4.00	2.5999	0.04700	2.8796	0.18194
4.25	2.7232	0.04154	3.0485	0.18483
4.50	2.8459	0.03512	3.2208	0.18644
5.00	3.0895	0.02012	3.5750	0.18493
5.50	3.3303	0.00234	3.9446	0.17802
6.00	3.5681	-0.02222		
6.50	3.8029	-0.04130		
7.00	4.0347	-0.06622		
7.50	4.2637	-0.09350		
8.00	4.4895	-0.12279		

where k_p is the stress intensity factor in the corresponding flat plate and is given by

$$k_p = \frac{N_0}{h} a^{\frac{1}{2}}, \quad \text{for } N_0 \neq 0, \ M_0 = 0$$

$$k_p = \frac{6M_0}{h^2} a^{\frac{1}{2}}, \quad \text{for } M_0 \neq 0, \ N_0 = 0 \tag{11}$$

The constants A_e and A_b are the extensional and bending components of the stress intensity factor and are given in Tables 1 and 2, either directly (A_e for $N_0 \neq 0$, $M_0 = 0$ and A_b for $N_0 = 0$, $M_0 \neq 0$) or through the following relations

$$A_b = \frac{3+v}{[\frac{1}{3}(1-v^2)]^{\frac{1}{2}}} a_b \quad \text{for} \quad N_0 \neq 0, \ M_0 = 0$$

$$A_e = [\tfrac{1}{3}(1-v^2)]^{\frac{1}{2}} a_e \quad \text{for} \quad N_0 = 0, \ M_0 \neq 0 \tag{12}$$

Regarding the results given by Tables 1 and 2, the following should be noted : a) the Poisson's ratio v appears explicitly as well as through λ in the expressions for k_{ij}. Thus the numerical results are obtained for one value of v only, which was selected to be $v = \frac{1}{3}$. b) Because of the assumption of Kirchhoff type boundary conditions in the formulation of the problem, the angular distributions of extensional and bending stresses around the crack tip are not the same, hence the superposition given by (10) is valid only for $\theta = 0$, that is, along the prolongation of the crack. c) The numerical analysis is carried out by using polynomial approximations for

TABLE 2

Stress intensity factor ratios for $N_0 = 0$, $M_0 \neq 0$

| λ	Cylinder		Sphere	
	a_e	A_b	a_e	A_b
0.2	0.006161	0.99816	0.00842	1.0020
0.4	0.01695	0.99340	0.02249	1.0070
0.6	0.02897	0.98660	0.03749	1.0137
0.8	0.04107	0.97846	0.05202	1.0211
1.0	0.05283	0.96946	0.06557	1.0287
1.2	0.06406	0.95986	0 07799	1.0364
1.4	0.07473	0.94993	0.08935	1.0439
1.6	0.08482	0.93976	0.09964	1.0512
1.8	0.09435	0.92956	0.10895	1.0583
2.0	0.1033	0.91936	0.11740	1.0652
2.2	0.1118	0.90923	0.12519	1.0718
2.4	0.1198	0.89926	0.13228	1.0783
2.6	0.1273	0.88940	0.13876	1.0845
2.8	0.1344	0.87970	0.14475	1 0905
3.0	0.1410	0.87023	0.15030	1.0964
3.25	0.1488	0.85863	0.15668	1.1035
3.50	0.1551	0.84740	0 16260	1.1103
3.75	0.1628	0.83643	0.1681	1.1170
4.00	0.1691	0.82440	0.1732	1.1233
4.25	0.1750	0.81542	0.1780	1.1297
4.50	0.1803	0.80539	0.1826	1.1357
5.00	0.1903	0.78616	0.1905	1.1470
5.50	0.2005	0.76832	0.2000	1.1580
6.00	0.2068	0.75079		
6.50	0.2137	0.73446		
7.00	0.2200	0.71879		
7.50	0.2255	0.7080		
8.00	0.2306	0.6897		
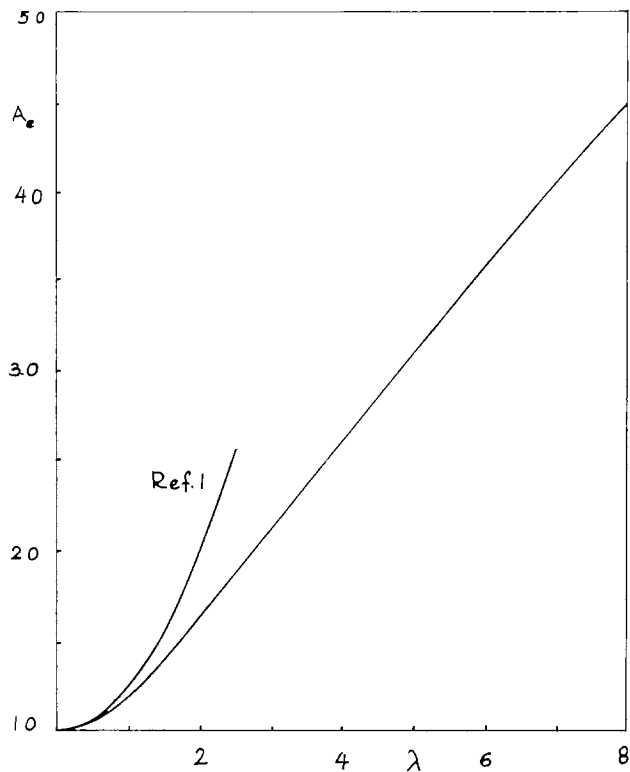
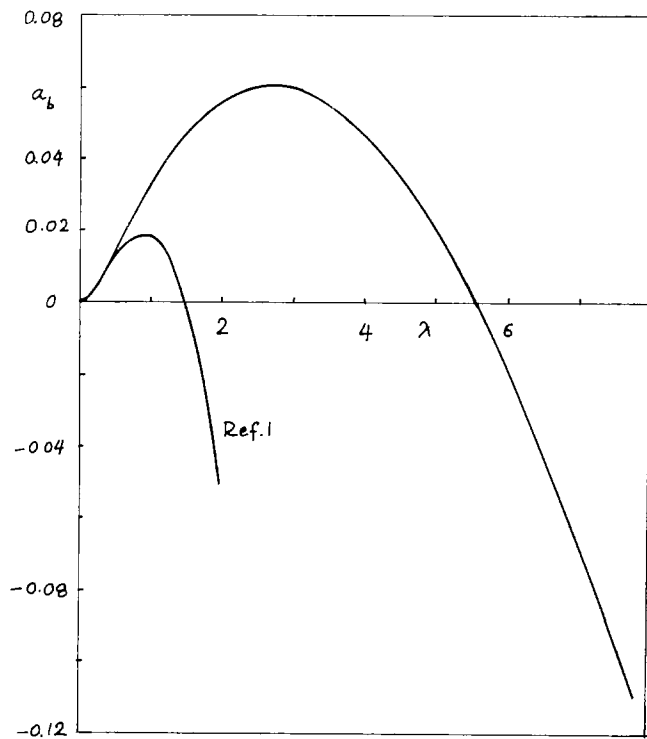Figure 1. Stress intensity ratio in cylinder $(N_0 \neq 0, \ M_0 = 0)$.

Figure 2. Stress intensity ratio in cylinder $(N_0 \neq 0, \ M_0 = 0)$.

Kelvin functions which are valid in $-8 \leqslant x \leqslant 8$ with a residual error of less than 10^{-7}, x being the argument of the functions. In the cylindrical shells, the argument x varies in $0 \leqslant x \leqslant \lambda$, and in spherical shells, in $0 \leqslant x \leqslant \lambda/2$. Since we required only four significant digit accuracy in the calculated quantities, technically, we could obtain useful results for values of λ somewhat larger than 8 in cylinders and 4 in spheres. To obtain more reliable results for higher values
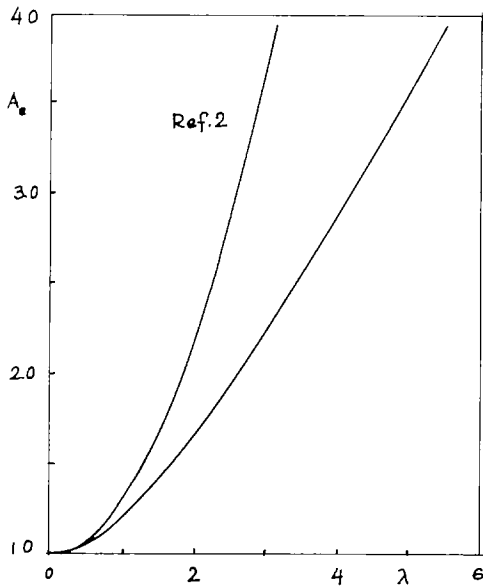
Figure 3. Stress intensity ratio in sphere $(N_0 \neq 0, \ M_0 = 0)$.
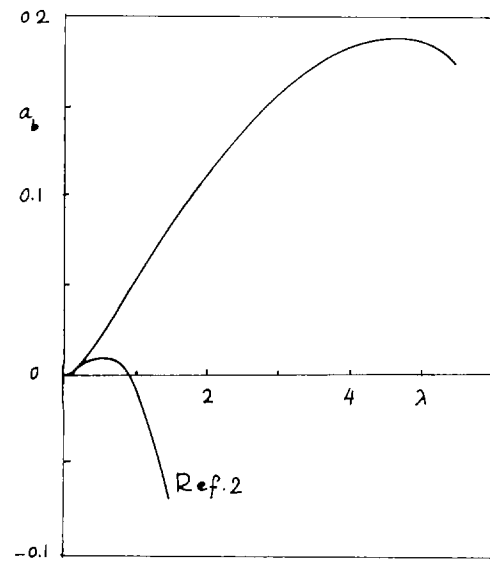
Figure 4. Stress intensity ratio in sphere $(N_0 \neq 0, \ M_0 = 0)$.
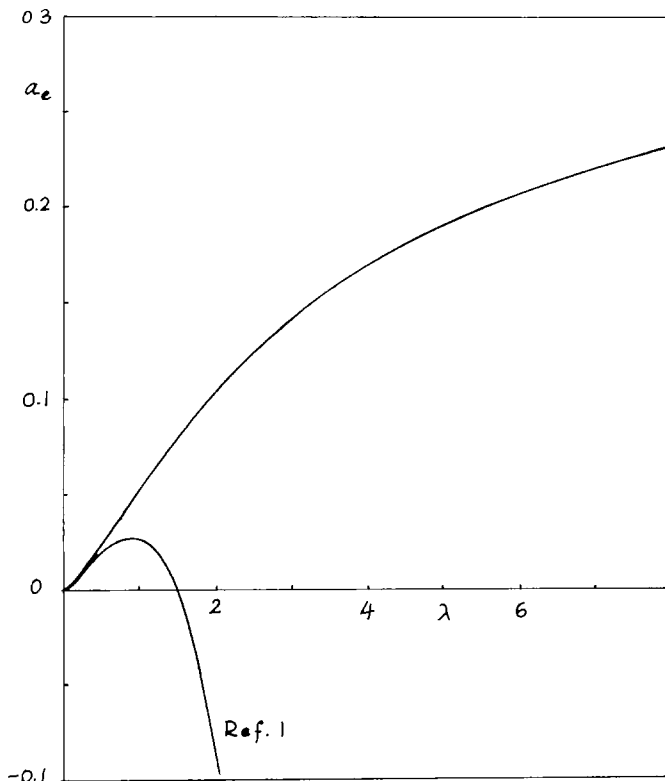

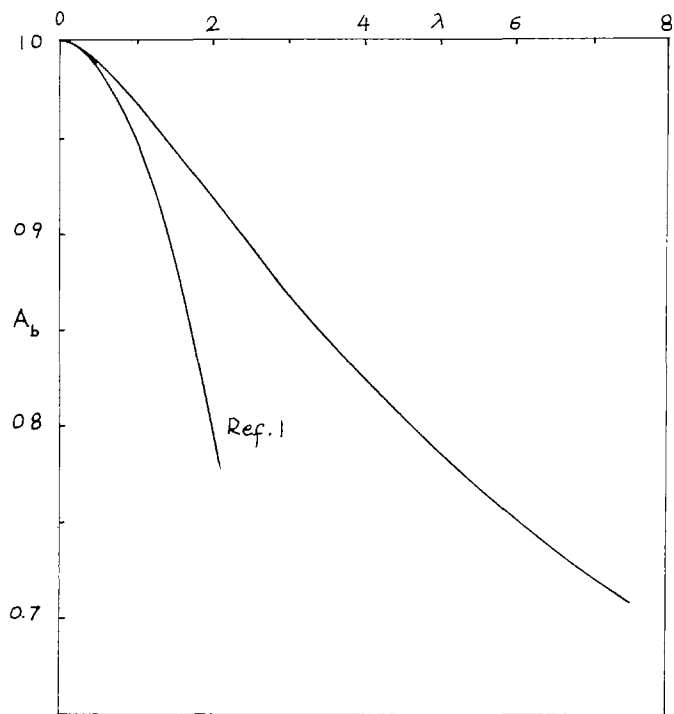Figure 5. Stress intensity ratio in cylinder $(N_0 = 0, \ M_0 \neq 0)$.

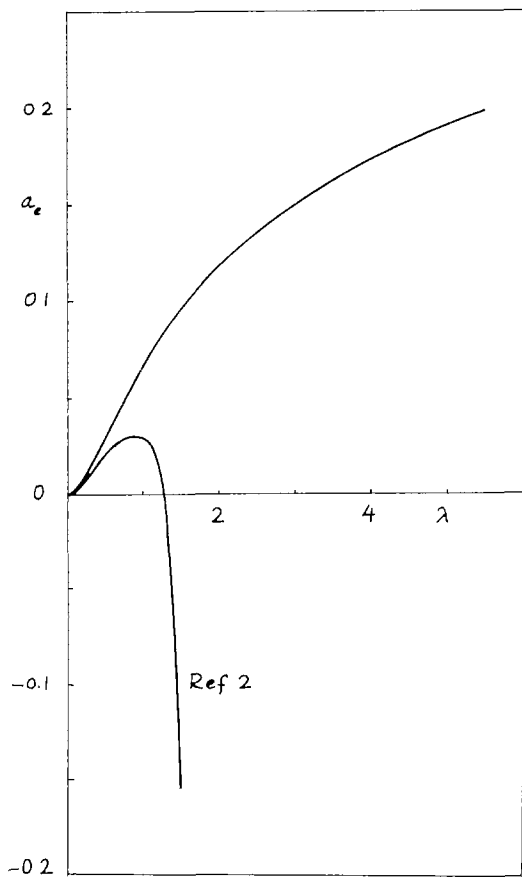Figure 6. Stress intensity ratio in cylinder $(N_0=0, M_0 \neq 0)$.

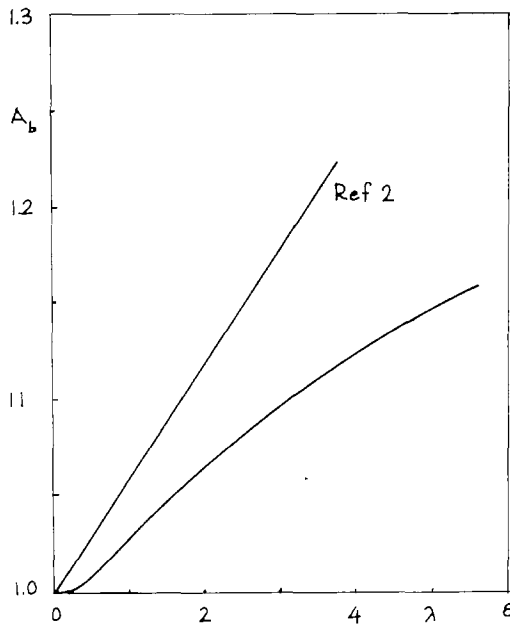Figure 7. Stress intensity ratio in sphere $(N_0=0, \; M_0 \neq 0)$.

Figure 8. Stress intensity ratio in sphere ($N_0 = 0$, $M_0 \neq 0$).

of λ, in addition to polynomial approximations valid for small x, one can also introduce the asymptotic expressions for the Kelvin functions valid for $|x| > 8$ (also given in ref. [7]).

The results given in Tables 1 and 2 are shown in Figs 1–8. The figures also include the results of the asymptotic solutions obtained in refs. [1] and [2].

Comparison of the two sets of curves clearly indicates the inadequacy of the asymptotic solutions for moderately large values of λ. Note that at $\lambda = 0$, as expected, all stress intensity ratio curves have zero slope. Note also that the effect of shell curvature on the stress intensity factors is much more significant if the shell is subjected to membrane loading rather than bending.

REFERENCES

[1] E. S. Folias, *Int. J. Frac. Mech.*, 1 (1965) 104.
[2] E. S. Folias, *Ibid.*, 1 (1965) 20.
[3] K. Marguerre, *Proc. 5th Int. Congr. Appl. Mech.*, 93 (1938).
[4] E. Reissner, *Proc. 1st Symp. Naval Struc. Mech.*, Pergamon, 74 (1960).
[5] E. S. Folias, ARL 64-174, Aerospace Research Labs., Office of Aerospace Research, USAF, October 1964.
[6] E. S. Folias, ARL 64-23, Aerospace Research Labs., Office of Aerospace Research, USAF, January 1964.
[7] M. Abramowitz and I. A. Stegun, Handbook of Mathematical Functions, Natl. Bur. Stds., *Appl. Math. Ser.* 55, 1964.
[8] N. I. Muskhelishvili, *Singular Integral Equations*, P. Noordhoff, Groningen (1953).
[9] W. Pogorzelski, *Integral Equations and Their Applications*, 1, Pergamon (1966).
[10] F. Erdogan, To appear in *SIAM J. Appl. Math.*, (1969).

RÉSUMÉ

On considère le problème symétrique d'enveloppes cylindriques et sphériques comportant une fissure qui se développe suivant un méridien. La solution est apportée dans le cas d'une contrainte de membrane uniforme et d'un moment de flexion uniformément appliqué aux lèvres de la fissure.

Ces composantes de traction et de flexion qui agissent sur le facteur d'intensité des contraintes sont déterminées en fonction des paramètres de l'enveloppe, et présentées sous forme de tableaux. Les résultats ont été également portés en diagrammes, de manière à les comparer aux solutions asymptotiques existantes.

ZUSAMMENFASSUNG

Das symmetrische Problem für zylindrische und sphärische Schalen, die einen meridionalen Riß haben, wurde behandelt. Das Problem wurde für eine einheitliche Membranlast und ein einheitliches Biegungsmoment auf der Oberfläche des Risses angewandt, gelöst.

Die ausdehnenden und biegenden Komponente des Druckstärkefaktorenradius wurden als Funktionen des Schalenparameters erhalten und tabuliert. Die Ergebnisse wurden auch aufgezeichnet, um sie mit den bestehenden asymmetrischen Lösungen zu vergleichen.